Identification of Phosphatidylserine and Phosphatidylcholine in Calcium-Induced Phase Separated Domains†

S. W. Hui,* L. T. Boni, T. P. Stewart, and T. Isac

ABSTRACT: Morphological changes associated with calcium-induced phase separation in mixed bovine brain phosphatidylserine (PS) and dipalmitoylphosphatidylcholine (DPPC) multilamellar vesicles were investigated by freeze–fracture electron microscopy, differential scanning calorimetry, X-ray diffraction, microprobe X-ray analysis, and ^{31}P NMR. Dipalmitoylthionphosphatidylcholine was substituted for DPPC to label PC in ^{31}P NMR and microprobe studies. Up to 25% of PS, there was no detectable morphological segregation induced by 20 mM Ca^{2+}. However, microprobe analysis showed that there were laterally separated PC- and Ca-rich domains within the same vesicles. The motion of phosphorus in PS, as observed by ^{31}P NMR, was selectively restricted by Ca^{2+}. The increasing lamellar repeat spacings with increasing PS percentage also implied the formation of DPPC-enriched domains. Between 30 and 50% PS and in excess of 20 mM Ca^{2+}, small cochleates were observed to roll out of the surfaces of multilamellar vesicles. The majority of the samples were in the form of small cochleates and small vesicles. X-ray diffraction showed the coexistence of both types of structures. Microprobe analysis showed that calcium and sulfur preferentially associated with cochleates and small vesicles, respectively, in samples containing thionphosphatidylcholine. The results suggested that 30% PS was the critical concentration at which macroscopic structural changes occurred. PS was sequestered by calcium from multilamellar vesicles to form PS-enriched cochleates, resulting in a corresponding enrichment of DPPC in the remaining small vesicles. Presumably, the macroscopic morphological segregation occurred only when the microscopic domains extended beyond a given critical size.

The structual phases of some negatively charged phospholipids are strongly affected by the presence of calcium (Jacobson & Papahadjopoulos, 1975). In some cases the presence of excess calcium can alter the interlamellar interaction resulting in gross morphological changes (Papahadjopoulos et al., 1974; Van Dijck et al., 1978). Calcium can induce phase separation of negatively charged lipids in mixed systems containing neutral and negatively charged phospholipids, due to the preferential association of calcium with the negatively charged phospholipids (Van Dijck et al., 1978; Ito & Onishi, 1974). The calcium-induced change is also believed to be associated with the fusion process (Newton et al., 1978; Wilschut et al., 1980; Duzgunes et al., 1981). When phosphatidylserine (PS)[1] is mixed with phosphatidylethanolamine (PE), the addition of calcium can trigger the formation of a nonbilayer phase by sequestering PS from PE (Cullis & Verkeij, 1979). Through these reactions, calcium could play an important role in modulating the properties of biomembranes, which usually consist of mixtures of negatively charged and neutral lipids.

In a previous study (Stewart et al., 1979) we found that dipalmitoylphosphatidylcholine and bovine brain phosphatidylserine were miscible in the absence of calcium ions. The introduction of calcium ions is expected to alter the phase diagram by selectively interacting with PS, thus "sorting out" the PS molecules from the mixture. Previous studies have shown that the Ca–PS complex is translamellar (Papahadjopoulos et al., 1974; Newton et al., 1978) and thereby introduces morphological distortions which eventually lead to a separate structure. What still remains unclear is whether the lateral phase separation occurs before the formation of translamellar complex. How do the different structures separate from an initial mixture? Do different structures represent compositional segregation?

In this study, we have determined the phase changes in the presence of calcium by correlating results from calorimetry, ^{31}P NMR, X-ray diffraction, and freeze–fracture electron microscopy. In addition, we have localized the calcium in the calcium–PS complex by energy dispersive X-ray microprobe analysis. Using thionphosphatidylcholine as a label (Chupin et al., 1979), we have determined the phase state of PC and PS independently by ^{31}P NMR. The identification of molecular species with their phases helped us to correlate the morphology, composition, and molecular packing observations, thereby furthering our understanding of the mechanisms of calcium-induced phase separation and structural changes in mixed lipid bilayers.

Materials and Methods

Phosphatidylserine from bovine brain (PS) and dipalmitoylphosphatidylcholine (PC) were purified as described (Stewart et al., 1979). Mixed lipid samples, each containing a total of 20 μmol of lipids, were evaporated from a chloroform solution under vacuum, at 25 °C, for 10–20 min. Each dry lipid sample was then hydrated by the addition of 15 mL of buffer solution [100 mM NaCl, 2 mM L-histidine, 2 mM 2-[[tris(hydroxymethyl)methyl]amino]ethanesulfonic acid, and 20 mM $CaCl_2$, pH 7.4] at 45 °C and dispersed by vortexing for 10 min. The suspension was further equilibrated at 45 °C for 2 h and sedimented in an Eppendorf minicentrifuge in three aliquots. The pellets were used immediately for differential scanning calorimetry (DSC), freeze–fracture, and X-ray diffraction experiments.

1,2-Dipalmitoyl-*rac*-glycero-3-thionphosphocholine (DPSPC) was synthesized by the condensation of the diacylglycerol with phosphorus thiochloride ($PSCl_3$) and choline toluenesulfonate (Vasilenko et al., 1982). This latter compound was prepared by mixing 1 mol of choline chloride with 1 mol of toluenesulfonic acid. Water and hydrochloric acid were re-

† From the Department of Biophysics, Roswell Park Memorial Institute, Buffalo, New York 14263. *Received January 10, 1983.* This work was supported by Research Grant GM 28120 from the National Institutes of Health (to S.W.H.).

[1] Abbreviations: DSC, differential scanning calorimetry; DPPC, dipalmitoylphosphatidylcholine; PS, bovine brain phosphatidylserine; DPSPC, 1,2-dipalmitoyl-*rac*-glycero-3-thionphosphocholine; NMR, nuclear magnetic resonance; T_1, spin–lattice relaxation time.

0006-2960/83/0422-3511$01.50/0

moved by repeated evaporation with toluene. The choline toluenesulfonate was crystallized from acetone and dried in vacuum over P_2O_5. A sample of 1.41 mmol of 1,2-dipalmitoylglycerol, dissolved in 10 mL of ethanol-free chloroform containing 0.248 mL of dry triethylamine, was added at room temperature dropwise under N_2 within 5 min to 1.74 mmol of $PSCl_3$. The temperature was then raised to 45 °C for 30 min. After cooling, 1 mL of dry pyridine and 0.668 g of choline toluenesulfonate were added and stirred for 18 h. The reaction was stopped by adding 0.3 mL of water, and then the mixture was stirred for 30 min. Lipids were extracted from the reaction mixture with chloroform and successively washed with 3% Na_2HCO_3, 5% HCl, and water. The pure compound was isolated by passage through a small silicic acid column. The product showed only one spot by thin-layer chromatography. ^{31}P NMR of the product (in chloroform solution) showed only one peak, with no detectable contamination of phospholipids.

^{31}P NMR experiments of mixed DPSPC and PS suspensions were performed on a Bruker WP-200 NMR spectrometer operating at 81 MHz. Five to ten micromoles of lipid mixtures was placed in 10-mm sample tubes. The samples were allowed to equilibrate at given temperatures for at least 15 min. All spectra were taken under continuous broad band proton decoupling. A sweep width of 50 kHz was employed, 2K data points were collected, and between 30 000 and 180 000 scans per spectrum at a delay of 0.1–0.4 s between pulses were applied. A line broadening of 200 Hz was employed during signal enhancement.

Samples for microprobe energy dispersive X-ray analysis were washed 3 times in double-distilled water and rapidly dried on carbon stubs. Cochleates and vesicles were identified by secondary electron imaging. The energy dispersive X-ray spectra were collected from stationary 10-nm microbeam probing spots or from reduced scanning areas confined to selected local regions. The spectral intensities of phosphorus, sulfur, and calcium and the ratio P/S/Ca were averaged from at least 10 samplings for each type of structure by using $CaHPO_4$ and $CaSO_4$ as standards for normalization. The data were collected by a Kevex spectrometer attached either to a Hitachi H-600 or to a JEOL 35 scanning electron microscope.

The experimental procedures for DSC, freeze–fracture and negative-stain electron microscopy, and X-ray diffraction were previously described (Stewart et al., 1979; Hui et al., 1980; Hui et al., 1981a). Both glycerated samples and rapidly frozen samples by the sandwich-propane method (Hui et al., 1981b) were used in freeze–fracture experiments, with the results being similar.

Results

All samples are made in the presence of excess 20 mM calcium. Samples containing 0–20% PS in DPPC have a surface texture identical with those in the absence of calcium (Stewart et al., 1979). Vesicles in this composition range seen by freeze–fracture are always multilamellar vesicles throughout all temperatures and compositions. At compositions greater than or equal to 30% PS in DPPC, a new feature is seen. A small "jellyroll" type structure is seen coexisting with the multilamellar vesicles at compositions up to 60% PS in DPPC (Figure 1A). These jellyroll structures or cochleate cylinders have been previously described by Papahadjopoulos et al. (1974). The surface of the cochleate cylinder is smooth. The multilamellar vesicles present at this composition range have surface textures that are consistent with those seen in calcium-free vesicles, namely, banded textures as seen below the high temperature onset of the phase transition. Some aggregated small vesicles with a smooth surface are also seen. A hybrid structure consisting of a combination of a textured vesicle continuous with a smooth cochleate cylinder (Figure 1B) is seen among vesicles and small cochleates. The continuity between a cochleate and a vesicle is further illustrated in a negative-stained preparation (Figure 1D). At compositions greater than 60% PS in DPPC the only structures seen by freeze-fracture at all temperatures are aggregates of vesicles and cochleate cylinders. In general, the cochleates formed in mixed lipids are smaller than those formed with pure PS (Papahadjopoulos et al., 1974). The surface of the aggregated vesicles (and cochleates) is devoid of any texture at all temperatures studied. No obvious difference in morphology is observed when DPPC is substituted by DPSPC in mixtures containing PS (Figure 1C).

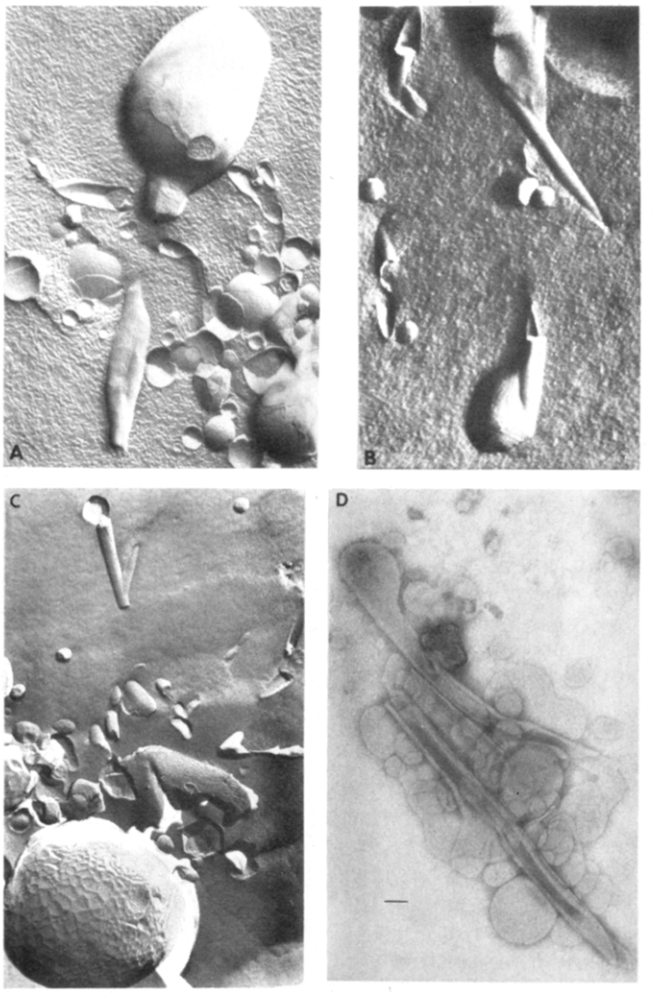

FIGURE 1: Freeze–fracture (A–C) and negative-stain (D) electron micrographs of PS and PC mixtures at room temperature in the presence of excess 20 mM Ca^{2+}. (A) 50% PS in DPPC; (B) 40% PS in DPPC; (C) 40% PS in DPSPC; (D) 40% PS in DPPC. Same magnification for all electron micrographs. Bar = 0.1 μm.

Microprobe analysis of individual vesicles and cochleates in samples containing 40% PS in DPPC in DPSPC shows that the respective P/Ca and P/S ratios are different for vesicles and cochleates. The results are given in Table I. The ratios measured from structures with similar morphological features do not vary by more than 20%, but those measured from different features of the same sample differ significantly. The Ca/P ratios in cochleates are slightly lower than the value of 0.5 expected from the bulk sample (assuming two PS's bind to one Ca), while the Ca/P ratios in vesicles are much lower than this value. The low Ca/P value (0.4) in pure PS co-

Table I: Elemental Distribution in Various Morphological Structures in Mixtures of PS and PC

bulk composition (mol %)			morphology[a]	ratios of normalized spectral intensity	
PS	DPSPC	DPPC		S/P	Ca/P
100			C		0.40 ± 0.01
40		60	C		0.31 ± 0.03
40	60		C	0.30 ± 0.05	0.29 ± 0.02
40		60	V		0.16 ± 0.03
40	60		V	0.88 ± 0.01	0.13 ± 0.01
20	80		V	0.85[b] ± 0.15	0.17[b] ± 0.07

[a] C = cochelates; V = vesicles. [b] Indicates large variations from area to area even on the same vesicles.

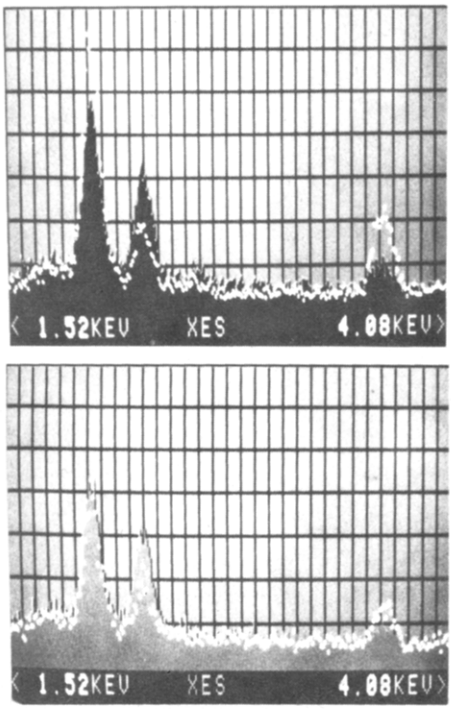

FIGURE 2: X-ray spectra from electron beam microprobe analysis. The three peaks from left to right represent the K-lines of P, S, and Ca, respectively, at 2.0, 2.3, and 3.7 eV. (Top) Samples containing 40% PS in DPSPC. White dots and black shade outline the typical spectra from cochleates and small vesicles respectively. (Bottom) Samples containing 20% PS in DPSPC. White dots and grey shade outline spectra from different areas (10-nm diameter) of a single vesicle.

chleates indicates the incomplete penetration of calcium into the lipid structure. The ratios are not affected significantly by substituting DPSPC for DPPC. The fact that calcium is also found in vesicles and sulfur in cochleates indicates that the phase separation is incomplete. Two typical spectra are shown in Figure 2 (top). Vesicles only are observed in samples containing 20% PS. The average P/S/Ca ratio is similar to that of the vesicles in samples containing 40% PS (Table I). However, when probed point-by-point, some variations in P/S/Ca ratio within the same vesicle are found. An example is given in Figure 2 (bottom). In any case, an increase in Ca/P ratio is usually accompanied by a decrease in the S/P ratio.

The differential scanning calorimetry traces of pure DPPC, pure PS, and various mixtures of the two in the presence of 20 mM Ca^{2+} are presented in Figure 3. The thermogram of pure DPPC in the presence of 20 mM Ca^{2+} is nearly identical with that in the absence of Ca^{2+}. The thermograms of pure PS in the presence of 20 mM Ca^{2+} shows no peak in the temperature range 0–70 °C (Jacobson & Papahadjopoulos, 1975). Presumably, the phase transition has been shifted to

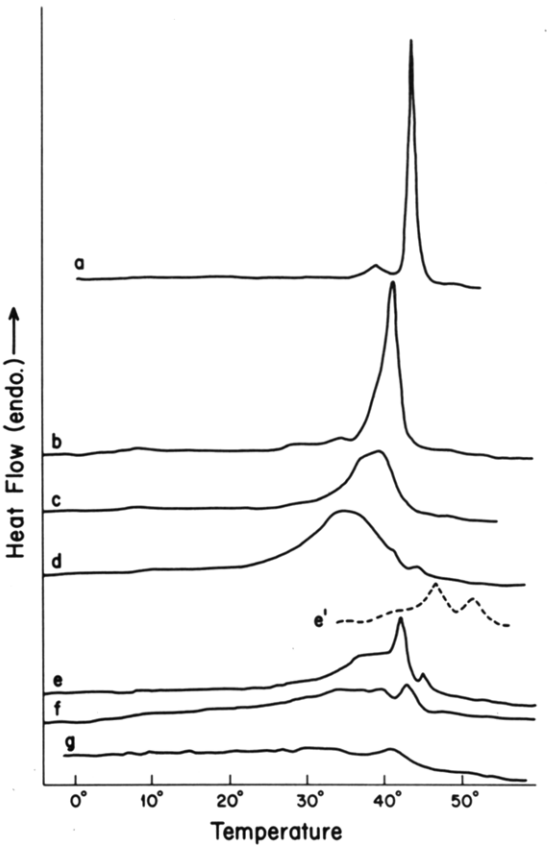

FIGURE 3: Differential scanning calorimetric tracings of mixtures of PS and DPPC prepared in the presence of 20 mM Ca^{2+}. Percentage of PS are (a) 0%, (b) 10%, (c) 20%, (d) 30%, (e) 40%, (f) 50%, (g) 70%, and (e′) 40% PS in DPSPC.

a temperature above this range. The thermograms of mixtures containing between 10 and 30% PS show the following trends: the peak heights are diminished and the widths are broadened; the main peak is shifted downscale. The thermogram of 30% PC yields a large broad peak that extends from 22.5 to 43 °C and is centered at approximately 35 °C with no detectable premelt. There is also a small peak detectable and centered at 44.5 °C. At a composition of 40% PS there is no longer a broad peak centered at 35 °C but a sharp peak centered at 42 °C with a broad shoulder that extends down to approximately 22 °C. The small peak that was evident at 30% phosphatidylserine is still evident but has been shifted upscale to approximately 45 °C. At 70% PS the thermogram shows a broad endotherm whose beginning and end points are difficult to determine. The thermal properties of DPSPC are very similar to those of DPPC, as shown by Vasilenko et al. (1982); the transition temperature of DPSPC (~44 °C) is slightly higher than that of DPPC (42.5 °C). The thermogram of 40% PS in DPSPC is plotted as a dashed line in Figure 3 for comparison. The shape of this thermogram is very similar to the corresponding one for 40% PS in DPPC, the peaks being 6 °C higher.

When excess calcium is added to sonicated PS vesicles, the ^{31}P NMR peak is broadened to over 200 ppm and is recoverable with a pulse interval of 20 s (Hope & Cullis, 1980). No resonance is detectable when pulsed at 0.1-s interval. This is due to the increasing T_1 as a result of motional restriction by the calcium–PS bonding (Hope & Cullis, 1980). However, when the same experiment is done with multilamellar PS vesicles, a small, broad peak is observed even if pulsed at 0.1-s interval, indicating a portion of PS has not interacted completely with calcium (results not shown). Figure 4 shows the

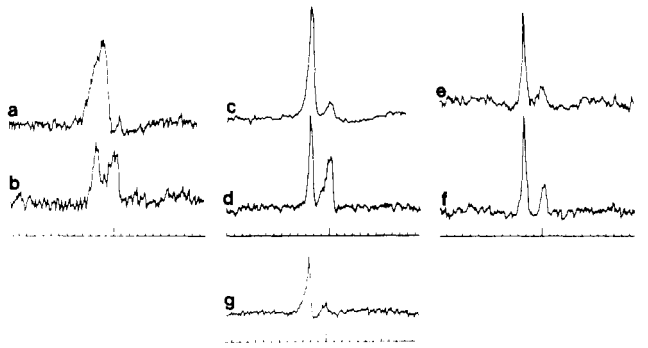

FIGURE 4: ^{31}P NMR spectra of mixtures of PS and DPSPC. Each scale division is 25 ppm, the long marker indicating the peak position for H_3PO_4. The higher peak from DPSPC is shifted by 55 ppm from the marker. (a, b) 40% PS, 20 °C; (c, d) 40% PS, 45 °C; (e, f) 20% PS, 50 °C. (b, d, f) Calcium-free samples; (a, c, e) samples containing 20 mM Ca^{2+}; (g) same as (e) but pulsed at 0.4-s interval.

^{31}P NMR spectra obtained from 20% and 40% PS in DPSPC suspended in aqueous buffer. In the absence of calcium, both PS and DPSPC resonances are about 50 ppm wide at or above 45 °C. The DPSPC resonance is shifted 55 ppm downfield from the PS resonance, in agreement with the spectrum of this thionphospholipid in chloroform solution. The spectral shape shown in Figure 4 is slightly distorted due to short pulse intervals applied (0.1 s) in order to economize experimental time. Spectra with typical "bilayer type" chemical shift anisotropy are obtainable from these samples when a 0.4-s pulse interval is applied. Such a spectrum is shown in Figure 4g. At 20 °C, the resonance peaks of both PS and DPSPC are broadened, indicating a L_α–L_β phase transition has taken place. The ratios of peak intensities of PS and DPSPC are roughly proportional to the compositions of the samples. The spectra of the same sample compositions in the presence of excess calcium (20 mM) show a considerable reduction in the size of the PS resonance peak at both temperatures. The residual peak indicates that a small portion of PS is not bound to calcium, due to the incomplete penetration of the calcium ion. The preferential broadening of the PS peak by calcium applies to samples containing 40% PS and, to a lesser extent, to samples containing 20% PS.

X-ray diffraction data are collected from the PS/DPPC and PS/DPSPC samples in excess of 20 mM Ca^{2+}. At PS concentrations less than 30%, where freeze–fractured samples showed only multilamellar vesicles, the low-angle diffraction of samples at temperatures below the phase transition onset always gives a series of lamellar reflections. The diffraction spacings are in the range 67–75 Å, depending on the composition. A single high-angle spacing of 4.2 Å ascribed to the gel phase lipid is also observed. The low-angle spacing increases with increasing PS percentage (Figure 5). Above the phase transition onset the low-angle spacing becomes 58–69 Å, while the high-angle diffraction becomes diffuse. When the freeze–fracture results show a coexistence of multilamellar vesicles and cochleate cylinders at a PS concentration between 30 and 50%, the low-angle diffraction shows two series of lamellar spacings at all experimental temperatures. One spacing ranged between 69 and 75 Å, and the other is always 53 Å. Two sharp high-angle spacings of 4.2 and 4.6 Å ascribed to the acyl chain packing in cochleates (Newton et al., 1978) are also observed. At PS concentrations greater than 50%, where the freeze–fracture observation shows a combination of small aggregated vesicles and cochleates, the low-angle diffraction always gives a single series of spacings at 53 Å with two sharp high-angle lines at 4.2 and 4.6 Å. A summary of low-angle diffraction data is presented in Figure 5. When

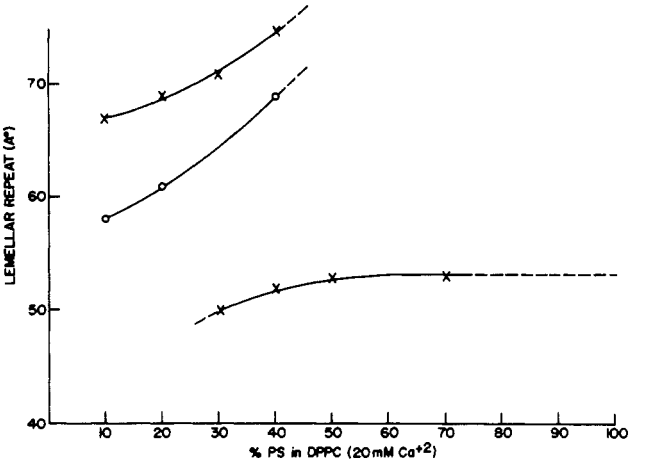

FIGURE 5: Small-angle X-ray diffraction spacings of mixtures of PS and DPPC in the presence of 20 mM Ca^{2+}. The (×) and (○) spacings were recorded below and above the onset temperature at which the 4.2-Å wide-angle diffraction line became undetectable. The cochleate spacings [lower (×)] were identified by an accompanied wide-angle line pair at 4.2 and 4.6 Å.

DPSPC is substituted for DPPC in 20% PS, the diffraction patterns are similar, although the lamellar repeat spacings are 5% smaller than the corresponding values for samples using DPPC at the same temperature. The difference in lamellar repeat spacings can be accounted for at least partly by the difference in transition temperatures of samples containing DPPC or DPSPC.

Discussion

According to our freeze–fracture and DSC results, the mixtures with compositions from 0 to 20% PS in the presence of 20 mM calcium appears to behave much like the mixtures without calcium. This observation implies that either calcium does not bind to PS at these compositions or the dilution of PS by a relatively high concentration of PC renders separate domains of PS–calcium complex too small to constitute a cooperative phase. Our NMR results show that these PS molecules bind to and are "solidified" by calcium, as indicated by the selective broadening of the PS but not the DPSPC ^{31}P NMR peaks by the addition of calcium. The PS/calcium binding at these low PS percentages is also supported by the fact that a considerable amount of calcium is detected by microprobe analysis. The uneven distribution, or the formation of PS/calcium domains at a scale not much larger than the microprobe spot size of 10 nm in diameter, in vesicles containing 20% of PS in DPSPC, is illustrated in Figure 2 (bottom). Areas containing higher sulfur from DPSPC are always associated with a lower calcium content, and vice versa. This observation gives direct evidence of a compositional lateral phase separation at a microscopic scale. The calcium ions in the interlamellar water space tend to draw the more or less evenly charged lamellae closer, thereby reducing the lamellae repeat from 74 Å in pure DPPC (in 20 mM Ca^{2+}) to 67 Å in samples containing 10% PS. As the concentration of PS increases, there is an increasing probability for PS to form small patches (domains) on the bilayer plane resulting from lateral phase separation induced by the calcium ions. The remaining lamellae are progressively enriched in DPPC, and the lamellae repeat tends to return to the value for pure DPPC. The scale of lateral phase separation is too small to be detected by DSC or by wide-angle X-ray diffraction. This model would explain our observation of the continuous increase in the lamellar repeat spacing with increasing PS content up to 30%.

At concentrations of 30–60% PS in DPPC, our results give

clear indications of structural separation. The appearance of cochleate cylinders at these compositions in freeze–fracture micrographs are indicative of segregation of PS by calcium. The low sulfur and high calcium contents in cochleates, and vice versa for small vesicles, support the postulate that the vesicles are enriched in PC and that most calcium is sequestered in cochleates. However, the composition segregation is not absolute. Judging from the sulfur content in cochleates from the 40% PS in DPSPC samples, and considering the lower Ca/P ratio in these cochleates than that in pure PS cochleates, we can estimate that these mixed lipid cochleates contain 25–30% DPSPC. On the other hand, the small vesicles in the same samples contain up to 88% of DPSPC. The Ca/P ratio in these vesicles apparently exceeds that expected from the remaining 12% PS. The excess calcium either binds to PC or is trapped within the vesicles. This explanation also applies to the excess calcium measured from samples containing 20% PS in DPSPC. The binding of calcium to DPSPC, however, does not affect the motion of the DPSPC molecules as does calcium to PS, as indicated by our ^{31}P NMR results.

We propose that the calcium first induces a limited lateral phase separation of the PS in the plane of the bilayer by forming cis PS–Ca complex domains; i.e., each calcium ion binds to two PS molecules on the same bilayer (Portis et al., 1979; Hoekstra, 1982). The PS is then free to roll into the cochleate structure in which calcium ions span the initially separated PS head groups of opposed bilayers, leaving little room for interlamellar water. During the rolling process, PS domains are laterally connected while PC-enriched domains are excluded. Eventually the cochleates separate totally from the multilamellar vesicle and become an independent structure. In the cochleates, the calcium and PS form a trans complex; i.e., a calcium ion binds to two PS molecules each on an opposite bilayer (Portis et al., 1979). The remaining vesicles are then enriched in PC, similar to those containing subcritical PS percentages (Table I). At this stage, the structures are sufficiently large to have cooperative behavior. The DSC traces at these compositions give two separate peaks. One peak appears to represent a PC-rich component, and the other peak represents a yet "unseparated" component. The phase transition of cochleates is beyond the temperature range of our DSC scans of (0–70 °C). The X-ray diffraction results support the coexistence of multilamellar vesicles and cochleate cylinders at the aforementioned compositions. We observed two series of low-angle spacings and two sharp high-angle spacings at these compositions. The 69–75-Å spacings are consistent with the lamellar repeat of multilamellar vesicles of hydrated bilayers at increasing PC concentrations in 20 mM Ca^{2+}, and the 53-Å spacings are indicative of a lamellar repeat of tightly packed, poorly hydrated bilayers which is typical of the cochleate type structures. The two sharp high-angle spacings of 4.2 and 4.6 Å are characteristic of the molecular packing in cochleate cylinders (Jacobson & Papahadjopoulos, 1975; Newton et al., 1978).

At compositions of greater than 60% PS in PC in 20 mM Ca^{2+}, only the diffraction from cochleates is seen. At these compositions the freeze–fracture shows aggregated small vesicles and cochleate cylinders. The highly curved surface of the small vesicles does not show the freeze–fracture textures that are characteristic of PC regardless of temperature. This result coupled with the results seen by DSC and X-ray diffraction is a clear indication of a calcium-induced structural separation. It appears that the vesicles are fragmented as a result of structural separation.

Freeze–fracture was again a very useful technique which supplied unique information. Even though the DSC and X-ray diffraction gave evidence for structural segregation, freeze–fracture gave direct observation for the spatial arrangement by which PS-enriched mixtures separated from the mixed lipid vesicles, through the "hybrid" cochleate–vesicle structures. The composition in each type of structure was determined by microprobe analysis. Making use of a DPSPC as a marker, this technique provided evidence for lateral phase separation even at low PS percentages (≤20%). ^{31}P NMR with a thionphosphatidylcholine label further identifies the physical states of each phospholipid species. The availability of thionphospholipids (Chupin et al., 1979; Vasilenko et al., 1982; Bruzik et al., 1982; Orr et al., 1982) opens up new means to identify molecular species in the physicochemical studies of phospholipids and membranes.

By applying five different techniques we have accumulated complementary information in the assignment of different phases for the mixtures of bovine brain phosphatidylserine and dipalmitoylphosphatidylcholine. In the absence of calcium, we have shown that these two lipids are completely miscible (Stewart et al., 1979). In the presence of calcium, we have found that there is a critical concentration of PS in DPPC for a structural separation to be effected. This concentration appears to be approximately 30% PS. Below this concentration, small, noncooperative domains are shown to exist in mixed bilayers. The studys of PS–Ca interaction in mixed lipid membranes will help us to understand the different degrees of phase separations and triggering mechanisms for structural transitions, which might serve as a model for control mechanisms in biomembranes.

Acknowledgments

Discussions and advice from Drs. D. Papahadjopoulos, J. Alderfer, and P. L. Yeagle at various stages of the project are appreciated. We thank Dr. Giese for the use of a Perkin-Elmer DSC-2 calorimeter and Dr. B. Eckert for the use of a JSM-35 scanning electron microscope and X-ray spectrometer.

Registry No. Dipalmitoylphosphatidylcholine, 2644-64-6; calcium, 7440-70-2; sulfur, 7704-34-9; phosphorus, 7723-14-0; 1,2-dipalmitoyl-*rac*-glycero-3-thionphosphocholine, 78599-45-8.

References

Bruzik, K., Gupte, S. M., & Tsai, M. D. (1982) *J. Am. Chem. Soc. 104*, 4682–4684.

Chupin, V. V., Vasilenko, I. A., Predvoditeleu, D. A., Sercbrennikova, G. A., & Evstigneeva, R. P. (1979) *Dokl. Akad. Nauk SSSR 248*, 235–237.

Cullis, P., & Verkleij, A. J. (1979) *Biochim. Biophys. Acta 552*, 546–551.

Duzgunes, N., Wilschut, J., Fraley, R., & Papahadjopoulos, D. (1981) *Biochim. Biophys. Acta 642*, 182–195.

Hoekstra, D. (1982) *Biochemistry 21*, 1055–1061.

Hope, M. J., & Cullis, P. R. (1980) *Biochem. Biophys. Res. Commun. 92*, 846–852.

Hui, S. W., Stwart, T. P., & Yeagle, P. L. (1980) *Biochim. Biophys. Acta 601*, 271–281.

Hui, S. W., Stewart, T. P., Yeagle, P. L., & Albert, A. D. (1981a) *Arch. Biochem. Biophys. 207*, 227–240.

Hui, S. W., Stewart, T. P., Boni, L. T., & Yeagle, P. L. (1981b) *Science (Washington, D.C.) 212*, 921–923.

Ito, T., & Onishi, S. (1974) *Biochim. Biophys. Acta 352*, 29–37.

Jacobson, K., & Papahadjopoulos, D. (1975) *Biochemistry 14*, 152–161.

Newton, C., Pangborn, W., Nir, S., & Papahadjopoulos, D.

(1978) *Biochim. Biophys. Acta 506*, 281-287.
Orr, G. A., Brewer, C. F., & Heney, J. (1982) *Biochemistry 21*, 3202-3206.
Papahadjopoulos, D., Poste, G., Schaeffer, B. E., & Vail, W. J. (1974) *Biochim. Biophys. Acta 352*, 10.
Portis, A. R., Newton, C., Pangborn, W., & Papahadjopoulos, D. (1979) *Biochemistry 18*, 780-790.
Stewart, T. P., Hui, S. W., Porties, A. R., & Papahadjopoulos, D. (1979) *Biochim. Biophys. Acta 556*, 1-16.
Van Dijck, P. W. M., de Kruijff, B., Verkleij, A. J., van Deenen, L. L. M., & de Gier, J. (1978) *Biochim. Biophys. Acta 512*, 84-96.
Vasilenko, I. A., de Kruijff, B., & Verkleij, A. J. (1982) *Biochim. Biophys. Acta 685*, 144-152.
Wilschut, J., Duzgunes, N., Fraley, R., & Papahadjopoulos, D. (1980) *Biochemistry 19*, 6011-6021.

Rearrangements of Chromatin Structure in Newly Repaired Regions of Deoxyribonucleic Acid in Human Cells Treated with Sodium Butyrate or Hydroxyurea†

Michael J. Smerdon

ABSTRACT: The rate and extent of redistribution of repair-incorporated nucleotides within chromatin during very early times (10–45 min) after ultraviolet irradiation were examined in normal human fibroblasts treated with 20 mM sodium butyrate, or 2–10 mM hydroxyurea, and compared to results for untreated cells. Under these conditions, DNA replicative synthesis is reduced to very low levels in each case. However, DNA repair synthesis is stimulated by sodium butyrate and partially inhibited by hydroxyurea. Furthermore, in the sodium butyrate treated cells, the core histones are maximally hyperacetylated. Using methods previously described by us, it was found that treatment with sodium butyrate had little or no effect on either the rate or the extent of redistribution of repair-incorporated nucleotides during this early time interval. On the other hand, there was a 1.7–2.5-fold decrease in the rate of redistribution of these nucleotides in cells treated with hydroxyurea; the extent of redistribution was unchanged in these cells. Since hydroxyurea has been shown to decrease the rate of completion of "repair patches" in mammalian cells, these results indicate that nucleosome rearrangement in newly repaired regions of DNA does not occur until after the final stages of the excision repair process are completed. Furthermore, hyperacetylation of the core histones in a large fraction of the total chromatin prior to DNA damage and repair synthesis does not appear to alter the rate or extent of nucleosome core formation in newly repaired regions of DNA.

It is now clear that rearrangements of chromatin structure take place following DNA repair synthesis in human cells damaged by ultraviolet (UV)[1] radiation (Smerdon & Lieberman, 1978, 1980; Smerdon et al., 1979, 1982a; Williams & Friedberg, 1979; Bodell & Cleaver, 1981; Cleaver, 1982) or UV-mimetic chemicals (Tlsty & Lieberman, 1978; Oleson et al., 1979; Zolan et al., 1982). Immediately after repair synthesis, the newly repaired DNA is rapidly digested to acid-soluble form by both staphylococcal nuclease and DNase I. This DNA is markedly reduced in nucleosome core particles and does not yield the familiar ~10-base repeat pattern on gels following digestion with DNase I. Subsequently, the newly repaired DNA becomes increasingly nuclease resistant, is associated with nucleosome cores, as well as histone H1, and yields an ~10-base repeat pattern following DNase I digestion (Smerdon & Lieberman, 1980; Smerdon et al., 1982a). These results led us to propose that this redistribution process, which we have termed "nucleosome rearrangement", may involve the refolding of newly repaired regions of DNA into their original (or near-original) nucleosome structures following a perturbation of these structures by the excision repair process (Lieberman et al., 1979). An alternative explanation for these results is that core histones are continuously changing their positions along the DNA ("sliding") and that damaged DNA bases are not "fixed" to their original positions within a nucleosome unit. The repair enzymes could then perform the excision of these lesions, as well as resynthesis, only when the lesions were "presented" in the linker region. The rearrangement that we observe would then be due to the continuous sliding of core histones in these newly repaired regions of DNA which would serve to randomize the distribution of this DNA between linker and core regions. We have classified this form of nucleosome rearrangement as "constitutive rearrangement", and it represents a marked contrast to the first proposal given above, which we have called "induced rearrangement" (Smerdon & Lieberman, 1978).

Data on the initial chromatin distribution and subsequent removal of labeled chemical adducts in intact cells support the induced rearrangement model (Oleson et al., 1979; Kaneko & Cerutti, 1980; Jack & Brookes, 1982). For example, the nonrandom distribution between linker and core DNA of the adducts formed by *N*-acetoxy-2-(acetylamino)fluorene (Kaneko & Cerutti, 1980) and *r*-7,*t*-8-dihydroxy-*t*-9,10-oxy-7,8,9,10-tetrahydrobenzo[*a*]pyrene (Jack & Brookes, 1982) remains unchanged for periods of 24–48 h in repair-deficient

† From the Biochemistry/Biophysics Program, Washington State University, Pullman, Washington 99164-4630. *Received January 5, 1983.* This study was supported by National Institutes of Health Grant ES 02614. M.J.S. is the recipient of a National Institutes of Health Research Career Development Award.

[1] Abbreviations: UV, ultraviolet; dThd, thymidine; Tris, 2-amino-2-(hydroxymethyl)-1,3-propanediol; BrdUrd, 5-bromo-2′-deoxyuridine; bp, base pair(s).

0006-2960/83/0422-3516$01.50/0